Journal of General Virology (2015), **96**, 210–219 **DOI** 10.1099/vir.0.069906-0

Quantitative assessment of prion infectivity in tissues and body fluids by real-time quaking-induced conversion

Davin M. Henderson,[1] Kristen A. Davenport,[1] Nicholas J. Haley,[2] Nathaniel D. Denkers,[1] Candace K. Mathiason[1] and Edward A. Hoover[1]

Correspondence
Edward A. Hoover
edward.hoover@colostate.edu

[1]Prion Research Center, College of Veterinary Medicine and Biomedical Sciences, Colorado State University, Fort Collins, CO 80523, USA

[2]Department of Diagnostic Medicine and Pathobiology, Kansas State University, College of Veterinary Medicine, Manhattan, KS 66506, USA

Prions are amyloid-forming proteins that cause transmissible spongiform encephalopathies through a process involving the templated conversion of the normal cellular prion protein (PrP^C) to a pathogenic misfolded conformation. Templated conversion has been modelled in several *in vitro* assays, including serial protein misfolding amplification, amyloid seeding and real-time quaking-induced conversion (RT-QuIC). As RT-QuIC measures formation of amyloid fibrils in real-time, it can be used to estimate the rate of seeded conversion. Here, we used samples from deer infected with chronic wasting disease (CWD) in RT-QuIC to show that serial dilution of prion seed was linearly related to the rate of amyloid formation over a range of 10^{-3} to 10^{-8} μg. We then used an amyloid formation rate standard curve derived from a bioassayed reference sample (CWD+ brain homogenate) to estimate the prion seed concentration and infectivity in tissues, body fluids and excreta. Using these methods, we estimated that urine and saliva from CWD-infected deer both contained 1–5 LD_{50} per 10 ml. Thus, over the 1–2 year course of an infection, a substantial environmental reservoir of CWD prion contamination accumulates.

Received 8 July 2014
Accepted 6 October 2014

INTRODUCTION

Prion diseases and many major human neurodegenerative diseases, including Alzheimer's disease, Parkinson's disease, amyotrophic lateral sclerosis, frontotemporal dementia and chronic traumatic encephalopathy, are associated with the misfolding of cellular proteins into an amyloid state (Frost & Diamond, 2010; McKinley *et al.*, 1983; Prusiner, 1998; Soto, 2012). In prion diseases, templated misfolding of the cellular prion protein (PrP^C) by an infectious, and potentially transmissible, β-sheet rich, amyloid form of the same protein, termed $PrP^{Sc,\ Res\ or\ D}$, is associated with neuronal loss and disease induction (Prusiner, 1998; Soto, 2012). Prion diseases are distinguished from other amyloid-associated diseases by the remarkable stability of the amyloid filaments formed and their transmissibility under natural conditions (Soto, 2012).

Detection of PrP^{Res} in the disease state can be accomplished by several methods. To date, immunohistochemistry and/or western blotting or animal bioassay have been considered the gold standards for the detection of PrP^{Res} (Bolea *et al.*, 2005). More recently, *in vitro* amplification methods [serial protein misfolding cyclic amplification (sPMCA) (Saborio *et al.*, 2001), amyloid seeding assay (ASA) (Colby *et al.*, 2007) and real-time quaking-induced conversion (RT-QuIC) (Atarashi *et al.*, 2011a)], all of which employ conversion of substrate PrP^C to the disease-specific conformation, have expanded the sensitivity and mechanistic possibilities of prion detection assays. For example, sPMCA, with its alternating cycles of elongation and sonication to facilitate fragmentation of nascent amyloid filaments, can be sufficiently sensitive to detect only a few molecules of PrP^{Res} (Castilla *et al.*, 2005a, 2008; Saá *et al.*, 2006; Saborio *et al.*, 2001). The ASA and RT-QuIC are generally analogous to sPMCA, but employ recombinant PrP^C instead of brain homogenate as substrate for disease-specific, *in vitro*, amyloid formation (Atarashi *et al.*, 2007, 2011a; Colby *et al.*, 2007). RT-QuIC offers the advantage of real-time assessment of amyloid fibril generation and has been successfully applied to many seed sources, some of which are available for antemortem sampling (Atarashi *et al.*, 2011a, b; Elder *et al.*, 2013; Haley *et al.*, 2013; Henderson *et al.*, 2013; McGuire *et al.*, 2012; Orrú *et al.*, 2011, 2014; Peden *et al.*, 2011; Sano *et al.*, 2013; Wilham *et al.*, 2010).

The prion hypothesis stipulates that an infectious PrP^{Res} seed serves as a template for the conversion of PrP^C. The RT-QuIC assay, as well as other *in vitro* assays, takes advantage of the replicative and amyloid seeding capacity of PrP^{Res}. Formation of amyloid is a nucleation-dependent

polymerization reaction (Baskakov & Bocharova, 2005; Knowles *et al.*, 2009). One would expect that increased concentration of seed would result in more frequent templating interactions and an increase in the formation of amyloid fibrils. Indeed, a feature of nucleated polymerization is that the addition of increasing concentrations of equal-sized seeds results in increasing rates of fibril formation (Cohen *et al.*, 2011; Knowles *et al.*, 2009). Mathematical models and experimental evidence demonstrate that nucleation-dependent polymerization substantially reduces the lag phase; when the spontaneous nucleation phase of polymerization is replaced by the addition of a seed, the elongation phase begins practically immediately (Cohen *et al.*, 2011; Harper & Lansbury, 1997; Knowles *et al.*, 2009). RT-QuIC records fibril formation by detection of an increase in fluorescence emission associated with the binding of thioflavin T (ThT) to the amyloid fibril. As with real-time (RT)-PCR, when faithful and exponential conversion occurs, the relationship between the initial seed (DNA or PrP^{Res}) quantity and rate of amplified product is linear (Gibson *et al.*, 1996; Murphy *et al.*, 1990; Pfaffl, 2001). Therefore, one would expect a linear relationship between the initial seed concentration and the rate of production of amyloid fibrils, as long as there is sufficient fibril content to produce a detectable ThT signal. Thus, we set out to better understand the relationship between amyloid seed concentration, ThT lag phase and concentration of infectious prions in biological samples using the RT-QuIC assay. Here, we calculated the rate (h^{-1}) at which detectable amyloid is formed from tissues and excreta of infected deer. We then related the reaction rate to prion infectivity by comparison with a reference bioassayed brain homogenate.

RESULTS

Reaction modelling and prediction

In order to quantify the relative amount of prion in a given sample using RT-QuIC, we applied a mathematical model to predict how the assay should behave. We hypothesized that the low levels of amyloid present at the early stage of the reaction would be below the detection limit of ThT fluorescence, which would prevent detection of amyloid formed in the early stage of the reaction (Fig. 1a). Therefore, the apparent lag phase observed by RT-QuIC likely reflects fluorescence detection limits, much like the early rounds of RT-PCR, when DNA replication is occurring yet no signal is observed (Murphy *et al.*, 1990). The amyloid seeding model also predicts that the time at which a sample becomes positive (the end of apparent lag phase) is linearly related to the concentration of seed. Therefore, upon serial dilution, a linear relationship should be observed when seed concentrations are plotted on a log scale (Fig. 1a). Here, we defined the rate of amyloid formation as the inverse of the time it takes for a reaction to reach the threshold (C_t), defined as the mean baseline

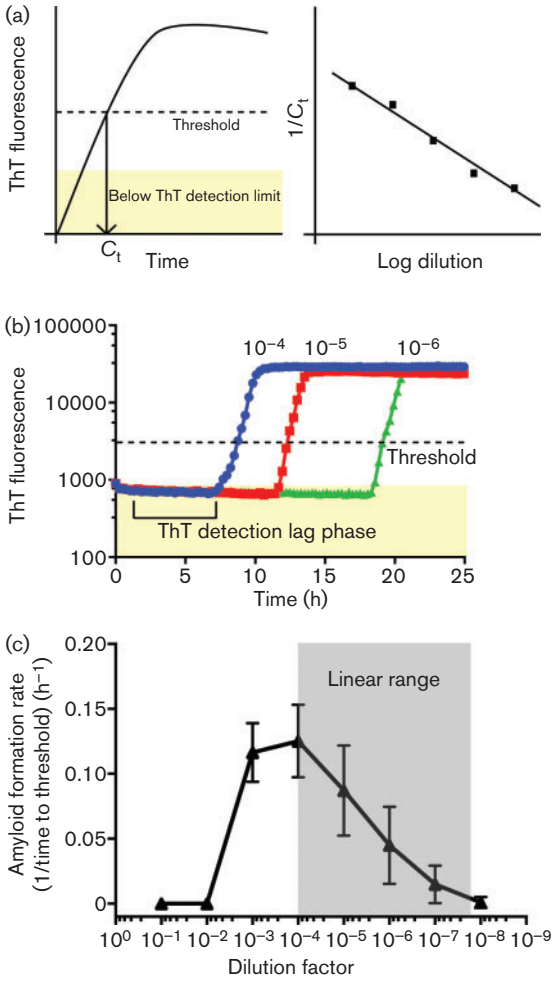

Fig. 1. Quantitative analysis of prion amyloid seeding levels with the RT-QuIC assay. (a) Model of the seeded RT-QuIC assay. Amyloid amplification is not observed until ThT fluorescence levels reach a detectable level. We estimate the amyloid formation rate by using the time at which a RT-QuIC assay crosses a defined threshold, termed C_t. When C_t values or the inverse of C_t values are plotted on a log scale, a linear relationship should be observed (Gibson *et al.*, 1996; Murphy *et al.*, 1990). (b) Reactions in the RT-QuIC assay were determined to be positive when a threshold of 5 SD above the initial fluorescence is reached. (c) Analysis of a CWD+ brain pool from 10^{-1} to 10^{-8} dilution of a 10% homogenate. The mean ± SD amyloid formation rate is displayed for each dilution. Each point is derived from eight replicates from three experiments. No reaction is observed at 10^{-1} or 10^{-2} and a slower reaction rate is seen at 10^{-3} dilution; 10^{-4} to 10^{-7} show a linear response as predicted.

fluorescence plus 5 SD. The rate (h^{-1}) of amyloid formation for serially diluted seeds is shown in Fig. 1(b). Essentially, a higher rate indicates that the reaction reaches the threshold and completion (all substrate consumed) faster. The inverse of C_t was plotted instead of C_t because some reactions do not reach the threshold during the length of the assay and therefore have no C_t that can be

plotted. To account for these samples, we conservatively assumed that negative reactions (those which did not reach our threshold for ThT fluorescence) have a C_t value approaching infinity and therefore have an amyloid formation rate of zero. All experiments included negative brain samples with corresponding dilutions and none of the negative samples met the criteria for positivity.

To investigate whether RT-QuIC behaved in accordance with the above model, we assayed a brain homogenate positive for chronic wasting disease (CWD+) over a wide serial dilution range (Fig. 1c). Interestingly, we routinely observed no positive reactions by RT-QuIC in 10^{-1} and 10^{-2} dilutions of 10 % CWD+ brain homogenates. Additionally, at 10^{-3} dilution, we observed a slightly slower rate of amyloid formation than with a 10^{-4} dilution. However, from 10^{-4} to the end point, we observed a linear response, as would be predicted from the seeded conversion model (Fig. 1c). We performed this analysis on 15 other brain homogenate samples (all from the obex region of the medulla of terminal CWD-infected deer) and observed a similar linear range for all the samples tested (data not shown). Thus, two phenomena were apparent: (1) RT-QuIC, as with other kinetic assays such as RT-PCR, has a linear range wherein defined assay conditions yield a linear response, and (2) reaction competitors or inhibitors were likely present in the lower dilutional range and their influence was eliminated upon serial dilution of the brain seed. This latter phenomenon has been observed previously in RT-QuIC and multiple other assays (Orrú *et al.*, 2011).

Elimination of competitors or inhibitors by phosphotungstic acid (PTA) precipitation

Next, we investigated the role of inhibitors in the RT-QuIC assay. As no reactions were positive at 10^{-1} and 10^{-2} dilution of a 10 % brain homogenate, we tested whether the addition of PTA precipitations of dilutions of the same homogenate could eliminate presumed inhibitors as demonstrated in previous work (Elder *et al.*, 2013; Henderson *et al.*, 2013). Indeed, when a 10^{-2} dilution of CWD+ brain homogenate was subjected to PTA precipitation, we observed positive RT-QuIC reactions (Fig. 2). Importantly, rates of amyloid formation at higher dilutions (10^{-3} and 10^{-4}) were not affected by the concentration of PTA in our assay conditions, consistent with previous work (Fig. 2) (Elder *et al.*, 2013; Henderson *et al.*, 2013). However, the addition of the PTA did not result in positive reactions when a 10^{-1} dilution of brain homogenate was tested (Fig. 2), suggesting that a fraction of the inhibitory factor(s) remained with PTA precipitated prions.

Comparing RT-QuIC reaction rate with western blot analysis of PrP^{Res}

To examine the range over which RT-QuIC could be quantitative, we analysed brain sections with high, intermediate and low levels of PrP^{Res}, as detected by western blotting. In two CWD-inoculated, terminally ill deer, proteinase K-resistant PrP^{Res} levels were demonstrated to be high in animal 776 and to be substantially lower in animal 783 (Fig. 3a). RT-QuIC analysis of the same brain sections was correlated with the western blot results; animal 776 had high levels of PrP^{Res} in the western blot and potent amyloid seeding activity, extending to a 10^{-8} dilution of obex, in RT-QuIC (Fig. 3b). Likewise, in deer 783, the lower level of PrP^{Res} in obex and mid-brain by western blot was correlated with ~100-fold lower amyloid seeding activity compared with deer 776 (783 obex end-point, 10^{-6}; 776 obex end-point, 10^{-8}; 783 mid-brain end-point, 10^{-4}; 776 mid-brain end-point, 10^{-7}) (Fig. 3a, b).

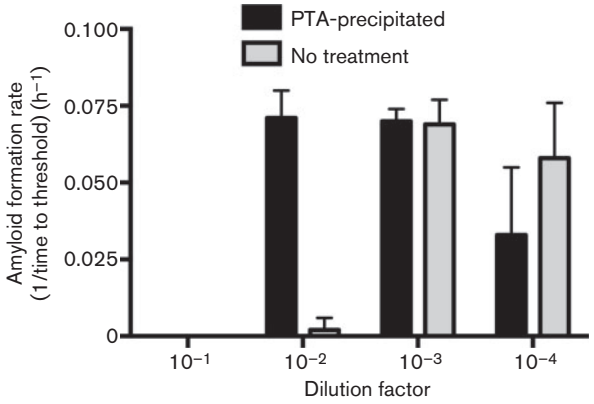

Fig. 2. PTA precipitation of CWD+ brain homogenate dilutions to enhance detection. The amyloid formation rate with or without PTA precipitation is shown for 10^{-1} to 10^{-4} dilutions of a 10 % CWD+ brain pool homogenate. No reaction is seen for 10^{-1} or 10^{-2} in non-PTA-precipitated samples. A 10^{-2} dilution from PTA-precipitated samples shows a similar amyloid formation rate to a 10^{-3} dilution of non-PTA-treated CWD+ brain. PTA precipitation does not substantially affect the amyloid formation rate of more dilute samples. Each result represents the mean ± SD and is derived from four replicates from two experiments.

Correlation of RT-QuIC reaction rate with infectivity

After establishing that CWD prions could be assayed over a multi-log range, we calculated the amyloid formation rates of a serially diluted CWD+ deer obex homogenate that had previously been analysed by cervid PrP transgenic mouse bioassay (Elder *et al.*, 2013). In the bioassay, the LD_{50} for the CWD+ brain homogenate was determined to be 13.8 pg or a 4.59×10^{-6} dilution of obex (Fig. 4a). The RT-QuIC amyloid formation rates were fit by semi-log linear regression and LD_{50} dose (13.8 pg) fell well within the linear assay range (Fig. 4b, intersection of dotted lines). The amyloid formation rate for 1 LD_{50} of obex (13.8 pg) was 0.0823 h^{-1} (Fig. 4b, intersection of the horizontal dotted line and the *y*-axis). The bioassay end-point dilution and the RT-QuIC standard curve were plotted on the same

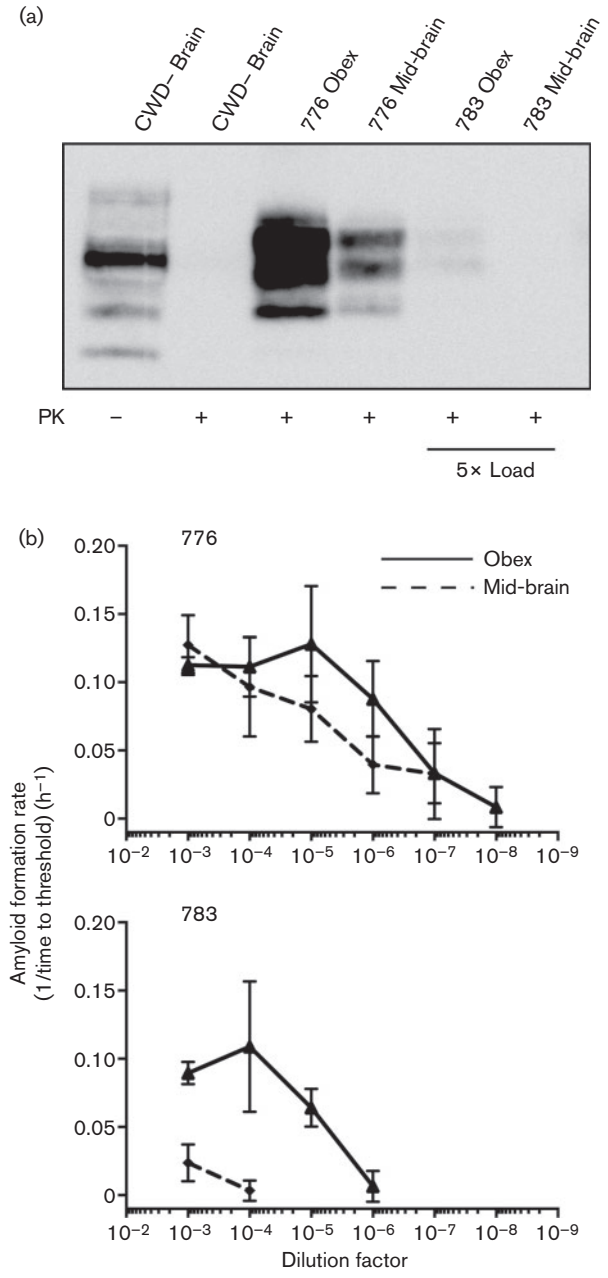

Fig. 3. PrP^{Res} levels detected by western blotting correlate with quantitative RT-QuIC assessment of the same sample. (a) Lanes 1 and 2, western blot analysis of CWD– brain sample with and without proteinase K (PK) treatment. Lanes 3 and 4, proteinase K-resistant PrP^{Res} samples from the obex and mid-brain of deer 776 that had advanced terminal disease. Lanes 5 and 6, corresponding samples from deer 783 that did not have robust accumulation of PrP^{Res} in any brain sample analysed. Five times the brain equivalents of lane 3 and 4 were added to lanes 5 and 6 so a signal could be observed. (b) Quantitative RT-QuIC analysis of the same brain samples shown in the western blot in (a). Both samples from deer 776 that had a robust western blot signal (lanes 3 and 4 above) had significant amyloid seeding capacity across more than five orders of magnitude. Both samples from deer 783 had less amyloid amplifying activity compared with 776. Each point represents the mean ± SD and is derived from four replicates from two experiments.

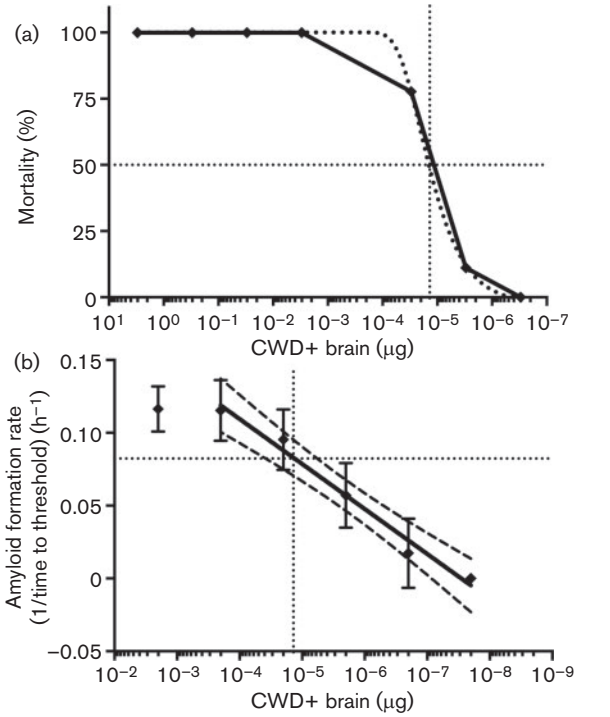

Fig. 4. Quantification of a CWD+ brain sample after the end-point dilution bioassay. (a) Percentage of cervidized transgenic mice that succumbed to CWD at each dilution point. Drop-lines (dotted) denote the LD_{50}. LD_{50} is calculated to be 13.8 pg. (b) RT-QuIC quantitative analysis of the same sample used for the end-point dilution bioassay in (a). The solid line is the best-fit semi-log linear regression of the bioassayed brain sample analysed by RT-QuIC. Dashed lines are the 95 % confidence intervals of the best-fit curve. The vertical dotted line is the LD_{50} (μg CWD+ brain). The horizontal dotted line is the calculated amyloid formation rate (h^{-1}) for 1 LD_{50}. Each point for RT-QuIC represents the mean ± SD and is derived from six replicates from three experiments.

x-axes (μg CWD+ obex). The detection limit of RT-QuIC was approximately two orders of magnitude more sensitive than the bioassay titration (Fig. 4a, b).

RT-QuIC estimation of CWD prion content of tissues of deer

In order to better understand the biological relevance of prion accumulation in peripheral tissues during the course of CWD infection, we determined the amyloid seeding activity and amyloid formation rates of serially diluted left ventricle, pancreas, jejunum and spleen. All these samples contained seeding activity over various dilution ranges (Fig. 5a), although all had less seeding activity than the obex of the same animal, as expected (Fig. 5a, dotted lines). The specific tissue samples presented here were strongly positive in a screen of all tissues from a terminally ill CWD+ white-tailed deer. Each sample selected showed substantial seeding activity and may not be a representative

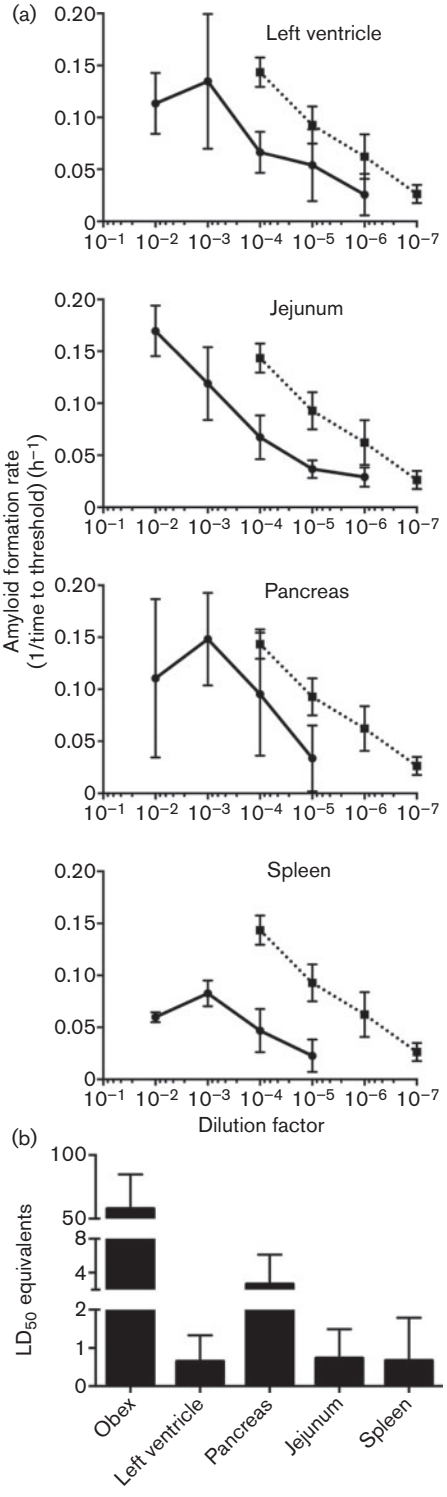

Fig. 5. Analysis and quantification of prion seeding activity in various tissues by RT-QuIC. (a) Amyloid formation rate determination over multiple log dilutions of left ventricle, jejunum, pancreas and spleen from a terminal CWD+ white-tailed deer. All tissues were harvested at terminal disease. The dotted line, which is the same in each panel, represents the rate values of the obex from the same animal. Each point represents the mean ± SD and is derived from four replicates from two experiments. (b) LD_{50} equivalents (mean ± SD) in 0.2 ng of obex, left ventricle, pancreas, jejunum and spleen.

of the prion load in the typical CWD disease course. Additionally, unidentified factors in the pancreas appear to increase variability in the amyloid formation rate in the RT-QuIC assay versus other tissues tested. These data are included in order to demonstrate the potential pitfalls in comparing divergent tissue samples using a single experimental protocol. We used the seeding activity of a 10^{-4} dilution (0.2 ng) of each tissue in the equation for the standard curve established in Fig. 4(b) [rate=0.031 log(μg sample)+0.23]. This calculation compares the seeding activity of the tissues to seeding activity of the bioassayed brain; in other words, brain equivalents for each tissue are derived (i.e. 0.2 ng spleen has the same amyloid formation rate, or the same seeding activity, as 1.16×10^{-4} ng obex). By dividing the brain equivalents by the bioassay-determined LD_{50} (13.8 pg), we were able to estimate the infectivity of the CWD prion dose in each tissue (Fig. 5b). The tissues tested had LD_{50} values ~50-fold lower than the obex sample, but were within the linear range of our assay conditions.

Estimation of prion concentrations in excreta of infected deer

As CWD is unique in its efficient horizontal transmission in nature, we applied the quantitative analysis described above to saliva and urine samples from a CWD-infected deer. Prions in body fluids and excreta are below detection limits with direct assays for prion detection in tissues. In addition, the presence of inhibitors in these complex biological fluids can pose additional complications for *in vitro* amplification assays (Castilla *et al.*, 2005b; Gonzalez-Romero *et al.*, 2008). As previously described for saliva (Henderson *et al.*, 2013), we used PTA precipitation to enrich for prions and to reduce reaction competitors in whole saliva. For urine, we used the low-speed pelleted fraction and subjected the resuspended pellet to PTA precipitation. We then compared the amyloid formation rate of obex from a given deer to saliva and urine from that animal collected longitudinally throughout the disease course (Fig. 6a). As anticipated, seeding activity in saliva and urine was substantially lower than in brain, but still within the linear range of the CWD+ obex reference curve (Figs 4a and 6a). We calculated the LD_{50} equivalents present in physiologically relevant volumes of excreta to estimate infectivity. We calculated that 10–20 ml of urine and 5–10 ml of saliva contained ~1 LD_{50} CWD prion infectivity (as assessed by transgenic mouse bioassay). It was evident that excreta contained substantial prion content, which may play a role in direct or indirect horizontal transmission of CWD.

DISCUSSION

We describe the mathematical relationship between the initial seed concentration and the amyloid formation rate observed in RT-QuIC. We have related the RT-QuIC

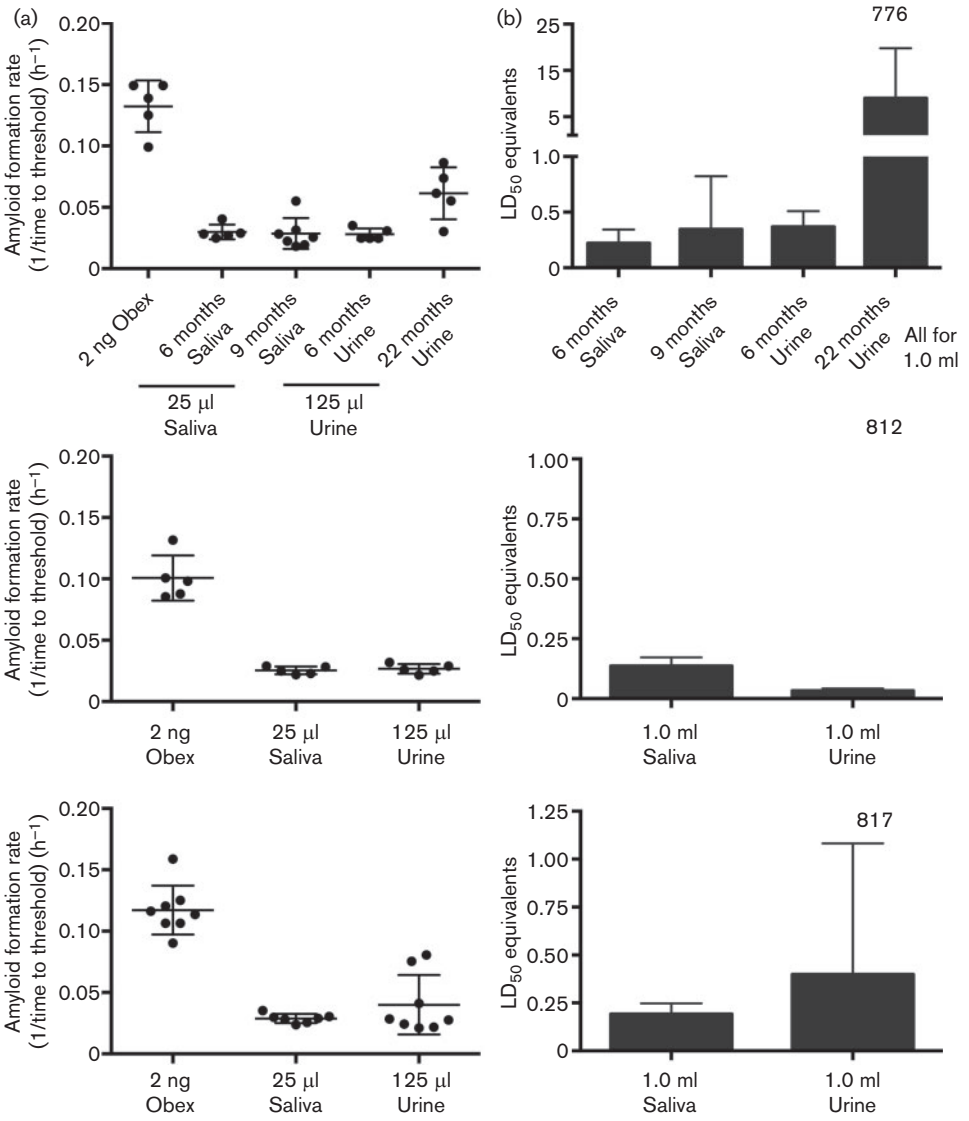

Fig. 6. Analysis and quantification of prion seeding activity in saliva and urine using RT-QuIC. (a) Amyloid formation rates from the obex, saliva and urine from the same animal. (Top) Two time points post-infection for saliva and urine (6 and 9 months for saliva; 6 and 22 months for urine) from deer 773 are shown. (Middle) Obex, saliva and urine from deer 812. (Bottom) Obex, saliva and urine from deer 817. Each dot represents one replicate. Each sample was analysed in at least two experiments. Bar, SD; centre line, mean. (b) Estimation of LD_{50} equivalents (mean ± SD) for 1.0 ml saliva and urine for the same samples in (a).

reaction rate to an LD_{50} determined by a transgenic mouse bioassay (Browning *et al.*, 2004) in order to estimate the relative infectivity/lethality of a given sample (Elder *et al.*, 2013). We have thus far analysed >20 samples and have derived the equivalent infectivity in all samples that fell within the linear range of the standard curve. Such calculations and comparisons allow for assessment of the relative levels of infectious prions present in peripheral tissues, body fluids and excreta compared with the central nervous system. This quantitative approach allows application of RT-QuIC to diverse biological materials and enables better understanding of peripheral prion accumulation during the course of infection. Moreover, quantification of the level of infectivity present in excreta could shed light on the spread of CWD though elk and deer populations, and give a more accurate picture of the reservoirs of infectious agent present in the environment and level of exposure required to transmit disease (Almberg *et al.*, 2011; Angers *et al.*, 2009; Denkers *et al.*, 2011, 2012; Haley *et al.*, 2009, 2011; Jennelle *et al.*, 2009; Mathiason *et al.*, 2006; Miller *et al.*, 2004; Perrott *et al.*, 2012; Saunders *et al.*, 2008; Sigurdson *et al.*, 1999; Spraker *et al.*, 1997; Tamgüney *et al.*, 2009; Williams & Young, 1980, 1982).

Our results are consistent with the formative work of Wilham *et al.* (2010), which estimated infectious prion

levels based on end-point dilution of seed. In addition, a standard curve based on amyloid formation rate instead of end-point dilution utilizes information from the whole dilutional series. We feel more confident using the whole dilutional series, as it is linear throughout and because the greatest variation is typically seen in the last dilutions to give positive reactions. The use of amyloid formation rate is therefore more amenable to the quantification of samples that have prion concentrations very near the end-point dilution, such as saliva and urine, which cannot be robustly serially diluted to find an end point. In considering the relationship between fibril formation rate and seed concentration, the present study in some ways parallels the work of Shi *et al.* (2013) who described a quantitative technique based on similar technology, but that relied on the mass of PrP^{Res}, as determined by western blotting. We extend these results by demonstrating that the data fit a previously described mathematical description of amyloid seeding and by the application of accepted quantitative methods used in other quantitative seeding assays, such as RT-PCR (Gibson *et al.*, 1996; Knowles *et al.*, 2009; Pfaffl, 2001).

The reaction and the mathematical calculations are based on the assumption that there are homogeneous mixtures of seed and substrate. Clearly, this is not the case in crude tissue homogenates or excreta in prion disease as it would be in DNA or RNA preparations. Multiple studies have demonstrated that there is a diverse population of prion aggregates present in the brain, which is likely true in other tissues as well (Prusiner *et al.*, 1980; Silveira *et al.*, 2005). By including multiple replicates and experiments, we typically yield linear best-fit models with R^2 values of >0.98, suggesting that uneven distribution of amyloid seed is not an insurmountable obstacle in the quantification of RT-QuIC assay results.

We have established a substantial linear range wherein quantification is possible using the RT-QuIC assay. However, inhibitors of an unknown nature are present in more concentrated samples (Figs 1 and 2). As with all assays, the amyloid formation rate must fall well within the linear range of the assay in order to accurately quantify a sample. Moreover, the best analysis would include multiple dilutions of each sample, and demonstration that the dilutions have a linear response and similar slope in the range assayed. Most samples give positive reactions over at least 3 log-fold dilutions; however, concentrations in samples such as saliva and urine may be sufficiently low to require concentration methods, such as PTA precipitation, to enable detection and reduce RT-QuIC reaction inhibitors (Fig. 2). Soto and colleagues, using sPMCA, previously reported that levels of prions shed in neat urine were approximately equivalent to a 10^{-10} to 10^{-11} dilution of brain (Gonzalez-Romero *et al.*, 2008). Therefore, based on our detection limits using the truncated (aa 90–231) Syrian hamster rPrP substrate, the likelihood of positive reactions over multi-log dilutions of excreta is reduced. Using a mean amyloid formation rate from PTA-precipitated excreta samples, we estimated an LD_{50} value for biologically relevant volumes of excreta. Our results are consistent with transgenic mouse bioassay studies where urine and saliva were found to contain infectious prions, but at levels low enough to be difficult to quantify by bioassay (Haley *et al.*, 2009; Kariv-Inbal *et al.*, 2006). We found that saliva contains more prion seeding activity than urine, which is also supported by previous bioassay studies (Haley *et al.*, 2009; Mathiason *et al.*, 2006). Future work to determine the nature of inhibitory factors, together with the exploration of new and more sensitive substrates, will permit more accurate quantification.

In summary, we have developed a mathematical framework for determining the relative amount of amyloid seed present in a given sample based on amyloid formation rate. We compared the RT-QuIC amyloid formation rate to the infectious dose of a bioassayed brain sample to estimate the infectivity of a given biological sample. This approach can be applied to assemble a quantitative picture of prion infectivity in peripheral tissues and excreta during infection, and ultimately may be useful for quantification of seeding activity in other amyloid-associated diseases, such as Alzheimer's disease, Parkinson's disease, amyotrophic lateral sclerosis and chronic traumatic encephalopathy.

METHODS

White-tailed deer. The Warnell School of Forestry and Natural Resources, University of Georgia, provided white-tailed deer, which were housed at the indoor CWD research facility at Colorado State University. All appropriate intuitional protocols for animal handling and treatment were followed. All animals with 800-series ID numbers were aerosol-exposed and received two 1 ml doses of a 5 % CWD+ brain homogenate intranasally (Denkers *et al.*, 2012). All deer with 700-series ID numbers were inoculated *per os* and received a single 1 g dose of CWD+ brain orally. Tissues were sourced from terminal necropsy from deer 816, which was inoculated through the aerosol route.

Tissue processing. Each tissue was harvested with a clean instrument to prevent cross-contamination. To produce 10 % homogenates, 0.05 g of each tissue was homogenized in 500 µl 1× PBS with a Blue Bullet bead-beater homogenizer (Next Advance). RT-QuIC analyses of tissues from two sham-inoculated CWD– animals were negative for every tissue analysed. Tissues were selected due to high levels of seeding activity and may not reflect typical levels found in CWD infection.

Protein expression and purification. Recombinant Syrian hamster PrP protein (aa 90–231) (SHrPrP) was produced in BL21 DE3 *Escherichia coli* via a plasmid kindly provided by Dr Byron Caughey. Overnight Express Auto induction (EMD Biosciences) was used to induce expression for ~24 h or until the final OD_{600} was at least 2.5. Bug Buster reagent and Lysonase (EMD Biosciences) were used for cell lysis, and inclusion body (IB) isolation was accomplished following the protocol included with the Bug Buster reagent (EMD Biosciences). All reagents for purification were purchased from Sigma-Aldrich. Purification was accomplished as described previously (Henderson *et al.*, 2013; Wilham *et al.*, 2010). In short, IB pellets from a 1 l culture were solubilized in 15 ml solubilization buffer (8.0 M guanidine hydrochloride, 100 mM $NaPO_4$, pH 8.0) and rotated for at least 1 h at room temperature. The solubilized IB pellet was applied to 20 ml Ni-NTA Superflow resin (Qiagen), which was washed and equilibrated in Denature buffer (6.0 M guanidine hydrochloride,

100 mM $NaPO_4$, pH 8.0). The solubilized SHrPrP protein was allowed to bind the resin for 45 min rotating at room temperature. The resin was then loaded on to a XK16-60 column (GE Healthcare) and put in line on a Bio-Rad Duoflow FPLC. Refolding was accomplished with a 180 ml gradient at 0.75 ml min^{-1} from Denature buffer to Refold buffer (100 mM $NaPO_4$, pH 8.0) followed by a 30 min wash with Refold buffer. Then, a 100 ml gradient elution from Refold buffer to Elution buffer (100 mM $NaPO_4$, 500 mM imidazole, pH 5.5) was applied to the column. All fraction tubes were prefilled with 2 ml Dialysis buffer (10 mM $NaPO_4$, pH 5.5). The elution peak was pooled and dialysed overnight at 4 °C against two changes of 4 l Dialysis buffer. A typical purification yielded 25 mg purified SHrPrP at a concentration of 0.4 mg ml^{-1}. Protein concentration was determined by taking the A_{280} and using an extinction coefficient of 25 900 in Beer's law.

RT-QuIC assay. Assay conditions were identical to those used previously [0.1 mg ml^{-1} ShrPrP, 1 × PBS (50 mM $NaPO_4$, 150 mM NaCl), 1.0 mM EDTA, 170 mM NaCl, 10 μM ThT] (Henderson *et al.*, 2013). The final salt concentration was 320 mM. Nunc optical bottom black 96-well plates and Nunc clear plate adhesive covers were used for all assays. Each RT-QuIC assay was performed for 250 cycles, for an assay time of ~62.5 h. A cycle comprised a 15 min shaking programme, wherein plates underwent 1 min of shaking at 700 r.p.m. using the double orbital setting followed by 1 min of rest. Next, a read programme was executed with an excitation setting of 450 nm and an emission setting of 480 nm. The gain was set to 1700 and each 96-well plate was read with 20 flashes per well with an orbital averaging of 4.

Analysis of excreta. Saliva samples were assayed as described previously (Henderson *et al.*, 2013). Aliquots of 100 μl neat saliva and 7 μl 4 % PTA (Sigma) were incubated at 37 °C for 60 min with shaking at 1500 r.p.m. The samples were then centrifuged at 17 000 ***g*** for 30 min. PTA pellets were resuspended in 20 μl 0.05 % SDS in 1 × PBS, pH 7.4 and subjected to the same RT-QuIC assay conditions as described above. Urine cell fraction pellets were obtained from 500 μl urine by centrifuging for 30 min at 15 000 ***g***. Pellets resuspended in 100 μl 1 × PBS with 7 μl 4 % sodium PTA solution were incubated at 37 °C for 60 min with shaking at 1400 r.p.m. Samples were then centrifuged for 30 min at 15 000 ***g*** and pellets were solubilized for 120 min in 16 μl 0.05 % SDS. Historical analysis of saliva and urine yielded 97.2 % (n=104) specificity for saliva and 99.3 % (n=280) specificity for urine. No CWD− urine or saliva sample ever yielded more than one false-positive replicate in a single experiment.

Amyloid formation rate and C_t calculation. C_t values were calculated by determining the time (h) when each positive reaction exceeded a threshold (5 SD above the mean initial florescence). We then took the inverse (1/time to threshold) of the time when the reaction reached the threshold; this value is the amyloid formation rate (h^{-1}). C_t values were calculated from at least two experiments and at least four replicates (per experiment) of each serial dilution between 10^{-2} and 10^{-8}. The linear range was typically between 10^{-2} to 10^{-4} and the loss of positivity (~10^{-6}). The linear range of each sample was fit with the equation $y=m\log(x)+b$ in order to interpolate 1 LD_{50} given the C_t value from the bioassayed tissue.

Western blotting. All appropriate samples were treated with proteinase K (50 μg ml^{-1}) at 37 °C for 1 h with shaking at 700 r.p.m. All samples were suspended in an equal volume of 2 × Lamelli SDS sample buffer and loaded into 12 % precast SDS-PAGE gels (Bio-Rad). Samples were electrophoresed at 190 V for 60 min, and transferred to PVDF membranes using standard settings and pre-purchased reagents in a Trans-Blot Turbo Transfer System (Bio-Rad). Detection was accomplished using the Snap-ID system from Millipore with the HRP-conjugated PrP-specific antibody BAR221.

ACKNOWLEDGEMENTS

This work was supported by the National Institutes of Health National Institute of Neurological Disorders and Stroke (grant R01 NS-061902) and by the Morris Animal Foundation (grant D12ZO-045). We thank Jeanette Hayes-Klug and Kelly Anderson for their excellent observation, care, and sample collection from deer, and Amber Mayfield for western blotting expertise.

REFERENCES

Almberg, E. S., Cross, P. C., Johnson, C. J., Heisey, D. M. & Richards, B. J. (2011). Modeling routes of chronic wasting disease transmission: environmental prion persistence promotes deer population decline and extinction. *PLoS ONE* **6**, e19896.

Angers, R. C., Seward, T. S., Napier, D., Green, M., Hoover, E., Spraker, T., O'Rourke, K., Balachandran, A. & Telling, G. C. (2009). Chronic wasting disease prions in elk antler velvet. *Emerg Infect Dis* **15**, 696–703.

Atarashi, R., Moore, R. A., Sim, V. L., Hughson, A. G., Dorward, D. W., Onwubiko, H. A., Priola, S. A. & Caughey, B. (2007). Ultrasensitive detection of scrapie prion protein using seeded conversion of recombinant prion protein. *Nat Methods* **4**, 645–650.

Atarashi, R., Sano, K., Satoh, K. & Nishida, N. (2011a). Real-time quaking-induced conversion: a highly sensitive assay for prion detection. *Prion* **5**, 150–153.

Atarashi, R., Satoh, K., Sano, K., Fuse, T., Yamaguchi, N., Ishibashi, D., Matsubara, T., Nakagaki, T., Yamanaka, H. & other authors (2011b). Ultrasensitive human prion detection in cerebrospinal fluid by real-time quaking-induced conversion. *Nat Med* **17**, 175–178.

Baskakov, I. V. & Bocharova, O. V. (2005). *In vitro* conversion of mammalian prion protein into amyloid fibrils displays unusual features. *Biochemistry* **44**, 2339–2348.

Bolea, R., Monleón, E., Schiller, I., Raeber, A. J., Acín, C., Monzón, M., Martín-Burriel, I., Struckmeyer, T., Oesch, B. & Badiola, J. J. (2005). Comparison of immunohistochemistry and two rapid tests for detection of abnormal prion protein in different brain regions of sheep with typical scrapie. *J Vet Diagn Invest* **17**, 467–469.

Browning, S. R., Mason, G. L., Seward, T., Green, M., Eliason, G. A., Mathiason, C., Miller, M. W., Williams, E. S., Hoover, E. & Telling, G. C. (2004). Transmission of prions from mule deer and elk with chronic wasting disease to transgenic mice expressing cervid PrP. *J Virol* **78**, 13345–13350.

Castilla, J., Saá, P., Hetz, C. & Soto, C. (2005a). *In vitro* generation of infectious scrapie prions. *Cell* **121**, 195–206.

Castilla, J., Saá, P. & Soto, C. (2005b). Detection of prions in blood. *Nat Med* **11**, 982–985.

Castilla, J., Morales, R., Saá, P., Barria, M., Gambetti, P. & Soto, C. (2008). Cell-free propagation of prion strains. *EMBO J* **27**, 2557–2566.

Cohen, S. I., Vendruscolo, M., Dobson, C. M. & Knowles, T. P. (2011). Nucleated polymerisation in the presence of pre-formed seed filaments. *Int J Mol Sci* **12**, 5844–5852.

Colby, D. W., Zhang, Q., Wang, S., Groth, D., Legname, G., Riesner, D. & Prusiner, S. B. (2007). Prion detection by an amyloid seeding assay. *Proc Natl Acad Sci U S A* **104**, 20914–20919.

Denkers, N. D., Telling, G. C. & Hoover, E. A. (2011). Minor oral lesions facilitate transmission of chronic wasting disease. *J Virol* **85**, 1396–1399.

Denkers, N. D., Hayes-Klug, J., Anderson, K. R., Seelig, D. M., Haley, N. J., Dahmes, S. J., Osborn, D. A., Miller, K. V., Warren, R. J. & other authors (2012). Aerosol transmission of chronic wasting disease in white-tailed deer. *J Virol* **87**, 1890–1892.

Elder, A. M., Henderson, D. M., Nalls, A. V., Wilham, J. M., Caughey, B. W., Hoover, E. A., Kincaid, A. E., Bartz, J. C. & Mathiason, C. K. (2013). *In vitro* detection of prionemia in TSE-infected cervids and hamsters. *PLoS ONE* **8**, e80203.

Frost, B. & Diamond, M. I. (2010). Prion-like mechanisms in neurodegenerative diseases. *Nat Rev Neurosci* **11**, 155–159.

Gibson, U. E., Heid, C. A. & Williams, P. M. (1996). A novel method for real time quantitative RT-PCR. *Genome Res* **6**, 995–1001.

Gonzalez-Romero, D., Barria, M. A., Leon, P., Morales, R. & Soto, C. (2008). Detection of infectious prions in urine. *FEBS Lett* **582**, 3161–3166.

Haley, N. J., Seelig, D. M., Zabel, M. D., Telling, G. C. & Hoover, E. A. (2009). Detection of CWD prions in urine and saliva of deer by transgenic mouse bioassay. *PLoS ONE* **4**, e4848.

Haley, N. J., Mathiason, C. K., Carver, S., Zabel, M., Telling, G. C. & Hoover, E. A. (2011). Detection of chronic wasting disease prions in salivary, urinary, and intestinal tissues of deer: potential mechanisms of prion shedding and transmission. *J Virol* **85**, 6309–6318.

Haley, N. J., Van de Motter, A., Carver, S., Henderson, D., Davenport, K., Seelig, D. M., Mathiason, C. & Hoover, E. (2013). Prion-seeding activity in cerebrospinal fluid of deer with chronic wasting disease. *PLoS ONE* **8**, e81488.

Harper, J. D. & Lansbury, P. T., Jr (1997). Models of amyloid seeding in Alzheimer's disease and scrapie: mechanistic truths and physiological consequences of the time-dependent solubility of amyloid proteins. *Annu Rev Biochem* **66**, 385–407.

Henderson, D. M., Manca, M., Haley, N. J., Denkers, N. D., Nalls, A. V., Mathiason, C. K., Caughey, B. & Hoover, E. A. (2013). Rapid antemortem detection of CWD prions in deer saliva. *PLoS ONE* **8**, e74377.

Jennelle, C. S., Samuel, M. D., Nolden, C. A., Keane, D. P., Barr, D. J., Johnson, C., Vanderloo, J. P., Aiken, J. M., Hamir, A. N. & Hoover, E. A. (2009). Surveillance for transmissible spongiform encephalopathy in scavengers of white-tailed deer carcasses in the chronic wasting disease area of Wisconsin. *J Toxicol Environ Health A* **72**, 1018–1024.

Kariv-Inbal, Z., Ben-Hur, T., Grigoriadis, N. C., Engelstein, R. & Gabizon, R. (2006). Urine from scrapie-infected hamsters comprises low levels of prion infectivity. *Neurodegener Dis* **3**, 123–128.

Knowles, T. P., Waudby, C. A., Devlin, G. L., Cohen, S. I., Aguzzi, A., Vendruscolo, M., Terentjev, E. M., Welland, M. E. & Dobson, C. M. (2009). An analytical solution to the kinetics of breakable filament assembly. *Science* **326**, 1533–1537.

Mathiason, C. K., Powers, J. G., Dahmes, S. J., Osborn, D. A., Miller, K. V., Warren, R. J., Mason, G. L., Hays, S. A., Hayes-Klug, J. & other authors (2006). Infectious prions in the saliva and blood of deer with chronic wasting disease. *Science* **314**, 133–136.

McGuire, L. I., Peden, A. H., Orrú, C. D., Wilham, J. M., Appleford, N. E., Mallinson, G., Andrews, M., Head, M. W., Caughey, B. & other authors (2012). Real time quaking-induced conversion analysis of cerebrospinal fluid in sporadic Creutzfeldt–Jakob disease. *Ann Neurol* **72**, 278–285.

McKinley, M. P., Bolton, D. C. & Prusiner, S. B. (1983). A protease-resistant protein is a structural component of the scrapie prion. *Cell* **35**, 57–62.

Miller, M. W., Williams, E. S., Hobbs, N. T. & Wolfe, L. L. (2004). Environmental sources of prion transmission in mule deer. *Emerg Infect Dis* **10**, 1003–1006.

Murphy, L. D., Herzog, C. E., Rudick, J. B., Fojo, A. T. & Bates, S. E. (1990). Use of the polymerase chain reaction in the quantitation of *mdr*-1 gene expression. *Biochemistry* **29**, 10351–10356.

Orrú, C. D., Wilham, J. M., Raymond, L. D., Kuhn, F., Schroeder, B., Raeber, A. J. & Caughey, B. (2011). Prion disease blood test using immunoprecipitation and improved quaking-induced conversion. *MBio* **2**, e00078-11.

Orrú, C. D., Bongianni, M., Tonoli, G., Ferrari, S., Hughson, A. G., Groveman, B. R., Fiorini, M., Pocchiari, M., Monaco, S. & other authors (2014). A test for Creutzfeldt–Jakob disease using nasal brushings. *N Engl J Med* **371**, 519–529.

Peden, A. H., McGuire, L. I., Appleford, N. E. J., Mallinson, G., Wilham, J. M., Orru, C. D., Caughey, B., Ironside, J. W., Knight, R. S. & other authors (2012). Sensitive and specific detection of sporadic Creutzfeldt–Jakob disease brain prion protein using real-time quaking-induced conversion. *J Gen Virol* **93**, 438–449.

Perrott, M. R., Sigurdson, C. J., Mason, G. L. & Hoover, E. A. (2013). Mucosal transmission and pathogenesis of chronic wasting disease in ferrets. *J Gen Virol* **94**, 432–442.

Pfaffl, M. W. (2001). A new mathematical model for relative quantification in real-time RT-PCR. *Nucleic Acids Res* **29**, e45.

Prusiner, S. B. (1998). Prions. *Proc Natl Acad Sci U S A* **95**, 13363–13383.

Prusiner, S. B., Groth, D. F., Bildstein, C., Masiarz, F. R., McKinley, M. P. & Cochran, S. P. (1980). Electrophoretic properties of the scrapie agent in agarose gels. *Proc Natl Acad Sci U S A* **77**, 2984–2988.

Saá, P., Castilla, J. & Soto, C. (2006). Ultra-efficient replication of infectious prions by automated protein misfolding cyclic amplification. *J Biol Chem* **281**, 35245–35252.

Saborio, G. P., Permanne, B. & Soto, C. (2001). Sensitive detection of pathological prion protein by cyclic amplification of protein misfolding. *Nature* **411**, 810–813.

Sano, K., Satoh, K., Atarashi, R., Takashima, H., Iwasaki, Y., Yoshida, M., Sanjo, N., Murai, H., Mizusawa, H. & other authors (2013). Early detection of abnormal prion protein in genetic human prion diseases now possible using real-time QUIC assay. *PLoS ONE* **8**, e54915.

Saunders, S. E., Bartz, J. C., Telling, G. C. & Bartelt-Hunt, S. L. (2008). Environmentally-relevant forms of the prion protein. *Environ Sci Technol* **42**, 6573–6579.

Shi, S., Mitteregger-Kretzschmar, G., Giese, A. & Kretzschmar, H. A. (2013). Establishing quantitative real-time quaking-induced conversion (qRT-QuIC) for highly sensitive detection and quantification of PrP^{Sc} in prion-infected tissues. *Acta Neuropathol Commun* **1**, 44.

Sigurdson, C. J., Williams, E. S., Miller, M. W., Spraker, T. R., O'Rourke, K. I. & Hoover, E. A. (1999). Oral transmission and early lymphoid tropism of chronic wasting disease PrP^{res} in mule deer fawns (*Odocoileus hemionus*). *J Gen Virol* **80**, 2757–2764.

Silveira, J. R., Raymond, G. J., Hughson, A. G., Race, R. E., Sim, V. L., Hayes, S. F. & Caughey, B. (2005). The most infectious prion protein particles. *Nature* **437**, 257–261.

Soto, C. (2012). Transmissible proteins: expanding the prion heresy. *Cell* **149**, 968–977.

Spraker, T. R., Miller, M. W., Williams, E. S., Getzy, D. M., Adrian, W. J., Schoonveld, G. G., Spowart, R. A., O'Rourke, K. I., Miller, J. M. & Merz, P. A. (1997). Spongiform encephalopathy in free-ranging mule deer (*Odocoileus hemionus*), white-tailed deer (*Odocoileus virginianus*) and Rocky Mountain elk (*Cervus elaphus nelsoni*) in northcentral Colorado. *J Wildl Dis* **33**, 1–6.

Tamgüney, G., Miller, M. W., Wolfe, L. L., Sirochman, T. M., Glidden, D. V., Palmer, C., Lemus, A., DeArmond, S. J. & Prusiner, S. B. (2009). Asymptomatic deer excrete infectious prions in faeces. *Nature* **461**, 529–532.

Wilham, J. M., Orrú, C. D., Bessen, R. A., Atarashi, R., Sano, K., Race, B., Meade-White, K. D., Taubner, L. M., Timmes, A. & Caughey, B. (2010). Rapid end-point quantitation of prion seeding activity with sensitivity comparable to bioassays. *PLoS Pathog* **6**, e1001217.

Williams, E. S. & Young, S. (1980). Chronic wasting disease of captive mule deer: a spongiform encephalopathy. *J Wildl Dis* **16**, 89–98.

Williams, E. S. & Young, S. (1982). Spongiform encephalopathy of Rocky Mountain elk. *J Wildl Dis* **18**, 465–471.